Optics and Laser Technology 104 (2018) 83–89

Contents lists available at ScienceDirect

Optics and Laser Technology

journal homepage: www.elsevier.com/locate/optlastec

Full length article

Novel report on SHG efficiency, Z-scan, laser damage threshold, photoluminescence, dielectric and surface microscopic studies of hybrid inorganic ammonium zinc sulphate hydrate single crystal

S.P. Ramteke [a,1], M.I. Baig [b], Mohd Shkir [c,d], S. Kalainathan [e], M.D. Shirsat [f], G.G. Muley [a], Mohd Anis [a,*,1]

[a] Department of Physics, Sant Gadge Baba Amravati University, Amravati 444602, Maharashtra, India
[b] Prof Ram Meghe College of Engineering and Management, Amravati 444701, Maharashtra, India
[c] Advanced Functional Materials & Optoelectronic Laboratory (AFMOL), Department of Physics, College of Science, King Khalid University, P.O. Box 9004, Abha 61413, Saudi Arabia
[d] Research Center for Advanced Materials Science (RCAMS), King Khalid University, P.O. Box 9004, Abha 61413, Saudi Arabia
[e] School of Advanced Sciences, Centre for Crystal Growth, VIT University, Vellore 632014, India
[f] RUSA Centre for Advanced Sensor Technology, Department of Physics, Dr. Babasaheb Ambedkar Marathwada University, Aurangabad 431005, Maharashtra, India

ARTICLE INFO

Article history:
Received 16 November 2017
Received in revised form 6 January 2018
Accepted 12 February 2018

Keywords:
Crystal growth
Inorganic materials
Dielectric studies
Optical studies
Microscopic studies

ABSTRACT

Hybrid inorganic nonlinear optical crystals find huge applications in laser assisted photonic devices therefore present communication firstly aims to investigate the dielectric, microscopic and linear-nonlinear optical properties of ammonium zinc sulphate hydrate (AZSH) crystal. The inorganic AZSH complex has been synthesized and $15 \times 10 \times 09$ mm^3 single crystal was grown by slow solvent evaporation method. The powder and single crystal X-ray diffraction technique has been employed to evaluate the crystalline phase and determine the structural parameters of AZSH crystal. The optical transparency of AZSH crystal has been examined within the wavelength rage of 200–1100 nm. The enhanced second harmonic generation efficiency of AZSH crystal is 2.53 times higher than standard KDP crystal. The laser damage threshold of AZSH crystal has been determined using the Nd:YAG laser operating at 1064 nm. The close and open aperture Z-scan studies have been performed to ascertain the nature of third order nonlinear optical (TONLO) refraction and absorption of AZSH crystal. The order of TONLO parameters n_2, β and χ^3 is found to be 10^{-9} cm^2/W, 10^{-4} cm/W, 10^{-4} esu respectively. The AZSH crystal is found to have violet colored luminescence emission centered at 370 nm. The dielectric constant and dielectric loss of AZSH crystal has been evaluated within 30 Hz to 1 MHz. The chemical etching technique has been imposed to examine the growth habitat and determine the etch pit density of AZSH crystal.

1. Introduction

In past few decades the development of new hybrid inorganic NLO crystals has been accelerated as they cater unique qualities such as wide transparency window ranging from far infrared to deep UV-region, huge mechanical stability, highly packed structural design, sufficient nonlinear response and large threshold to laser exposure which ultimately vitalize the credibility of these crystals for optoelectronics, photoemission spectroscopy, laser micromachining, semiconductor lithography, optical modulation, frequency shifting/conversion, optical switching and laser device applications [1–5]. The appealing technologically vital inorganic NLO crystals that are currently utilized in laser complied device applications at mass scale are MgO:$LiNbO_3$, $NH_4H_2PO_4$, $LiIO_3$, KH_2PO_4, KD_2PO_4, $CsLiB_6O_4$, $KNbO_3$, $KTiOAsO_4$, $CdGeAs_2$ [6,7]. Looking at the stimulating impetus of inorganic crystals across the globe attention of our group is focused to explore the unique class represented by the general formula $A_2B(XO_4)_2{\cdot}6H_2O$ where A corresponds to big univalent cations (K^+, NH_4^+, Rb^+, Cs^+, etc), B corresponds to smaller divalent cations (Ni^{2+}, Co^{2+}, Cu^{2+}, Mg^{2+}, Zn^{2+}, Fe^{2+}, etc) and X corresponds to the S, Se or Cr. El-Fadl et al. recently explored the structural, morphological and linear optical properties of potassium zinc sulfate hydrate (KZSH) and ammonium zinc sulfate hydrate (AZSH) single crystals [8]. However, from the application point of view the precise knowledge of second harmonic generation (SHG) efficiency, third order nonlinear optical parameters, laser damage threshold, luminescence, dielectric and microscopic surface properties are essential which are not reported in case of KZSH and AZSH crystals. In current investigation a novel report is put forth which deals to explore the most vital missing

* Corresponding author.
E-mail addresses: loganees@yahoo.com, loganees@gmail.com (M. Anis).
[1] These authors contribute equally to this work.

https://doi.org/10.1016/j.optlastec.2018.02.018
0030-3992/

properties of AZSH crystal by imposing structural, UV–visible, Kurtz-Perry test, Z-scan, laser damage threshold, photoluminescence, dielectric and chemical etching analysis to bring out the potential credibility of AZSH crystal for distinct NLO device applications.

2. Experimental procedure

2.1. Synthesis and crystal growth

In order to synthesize the AZSH complex the SDfine make ammonium chloride and zinc sulphate were dissolved in double distilled water in 1:1 M ratio and the mixture was allowed to stir on a constant speed for four hours to facilitate the homogeneous reaction of the reactants. The scheme of chemical reaction giving the product of AZSH is given below,

$$ZnSO_4 \cdot 6H_2O + (NH_4)_2SO_4 \xrightarrow{H_2O} (NH_4)_2ZnSO_4 \cdot 6H_2O \ (AZSH)$$

The mixture solution was filtered through the membrane filter paper using the vacuum pump. The filtrate was transferred in the clean rinsed beaker and it was placed in the vibration free constant water bath maintained at 35 °C. As the slow evaporation process begins the nucleation of seed crystal was observed and single crystals of appreciable size with well-defined faces were obtained within the period of two weeks. The as grown AZSH complex crystal of dimension 15 × 10 × 09 mm^3 is shown in Fig. 1a. The purity of AZSH material was achieved by repetitive recrystallization process.

2.2. Characterization techniques

The properties of AZSH crystal has been evaluated by different techniques as discussed: (a) Single crystal X-ray diffraction (XRD) analysis was performed by using Enraf Nonius CAD4 single crystal X-ray diffractometer, (b) powder XRD pattern analysis was recorded using the Bruker Advanced D8 powder X-ray diffractometer and indexing was done using the powderX software constraining the 2θ error limit to 0.01°, (c) Linear optical study was examined within 200–1100 nm using the Shimadzu UV-1061 spectrophotometer, (d) SHG efficiency was determined using the Nd:YAG laser (Q-switched mode, 1064 nm, 10 Hz, 6 ns), (e) Z-scan analysis was performed using the CW He-Ne laser operating at 632.8 nm and the optical resolution of components utilized in Z-scan setup is focal length of focusing lens = 20 cm, optical path distance = 113 cm, beam waist radius (ω_a) = 1 mm, aperture radius (r_a) = 1.5 mm, beam intensity at the focus (Io) = 2.3375 KW/m^2, (f) LDT was determined using the Nd:YAG laser (1064 nm, 10 ns, 10 Hz), (g) dielectric studies were carried out within frequency range of 30 Hz to 1 MHz using the HIOKI 3532 LCR cubemeter, (h) photoluminescence nature was examined using the Hitachi F-7000 fluorescence spectrophotometer with analysis method emission and excitation slit width = 1 nm, scan speed = 240 nm/min, delay = 0 s, response time = 0.1 s, (i) optical microscope Carl Zeiss was used to capture the microimage of crystal surface in reflection mode at resolution of 100 μm.

3. Results and discussion

The single crystal XRD data reveals that the title crystal belongs to the monoclinic crystal system oriented with the space group $P2_1/a$. The unit cell parameters of AZSH crystal are a = 9.235 (±0.013) Å, b = 12.516 (±0.007) Å, c = 6.248 (±0.002) Å, β = 106.89° and the volume V = 690.025 (±1.1) $Å^3$. These values match well with the reported data in ICDD PDF card No. 04-007-5463 confirming the formation of AZSH crystal. The powder XRD technique has been employed to examine the crystalline phase and purity of the AZSH crystal. The recorded PXRD pattern is shown in Fig. 1b. It is worth mentioning that the PXRD pattern and indexing match very well with reported PXRD pattern [8]. The sharpness/broadening of diffraction peaks give determinant clue about the crystalline quality of material [9]. In present study the AZSH crystal material offers sharp, narrow and high intensity diffraction peaks which are ideal feature of material exhibiting good crystalline nature and lesser density of defects and grain boundaries [10,11]. The crystals with lesser defect centers are eventually desirable for device fabrication.

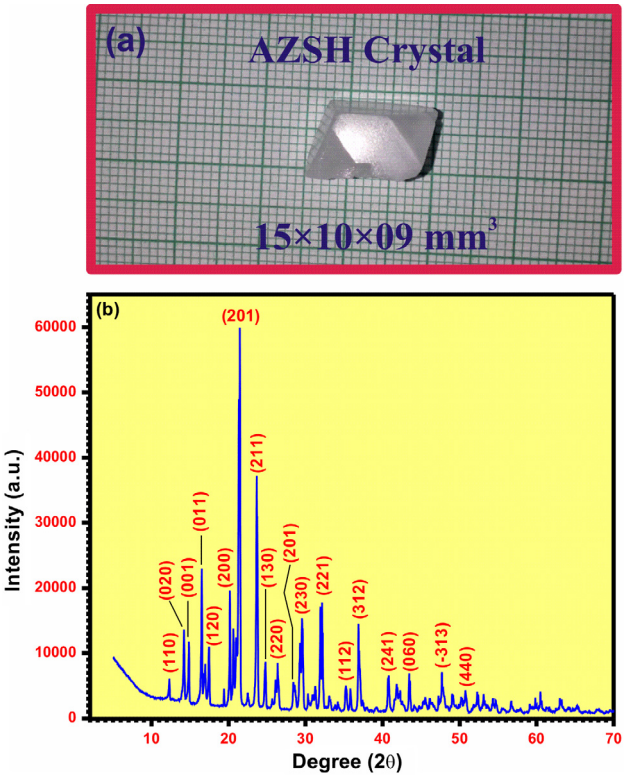

Fig. 1. (a) AZSH single crystal. (b) PXRD pattern of AZSH.

Thus the intrinsic and extrinsic factors that dwells the property of linear optical transmittance in crystal is governed by the electronic transition facilitated by the interaction of electromagnetic signal with material composition (atoms, ions, electrons) [12–14] while the limit of transmittance is determined by molecular anisotropy along the crystal plane and internal scattering/absorption from defects (grain boundaries, voids, cracks, bubbles, impurities, solvent inclusions) [15,16]. The designing of polarizer and lenses demand high quality and optically homogeneous crystal hence in order to testify that the optical transmittance of 1.5 mm thickness AZSH crystal has been recorded within 200–1100 nm as shown in Fig. 2a. It reveals that the AZSH crystal attributes the maximum transmittance up to 67% throughout the visible region. Interestingly the title crystal does not show any transition within visible region which might have been expressed due to lesser density of scattering centers in crystal medium [17] also the presence of Zn^{2+} ion offers high optical transparency in visible region owing to closed d^{10} shell electrons [18–20]. Thus wide operative wavelength range of AZSH crystal suggest its prime utility for designing components for transmission of 2nd/3rd harmonic signals derived from Nd:YAG laser [21] and UV-tunable lasers [22].

The most fundamental and essential condition for crystal to generate the SHG is to acquire the acentric symmetry and the Kurtz-Perry powder test [23] is the most reliable tool to determine the exact magnitude of the SHG efficiency of the given crystal. In

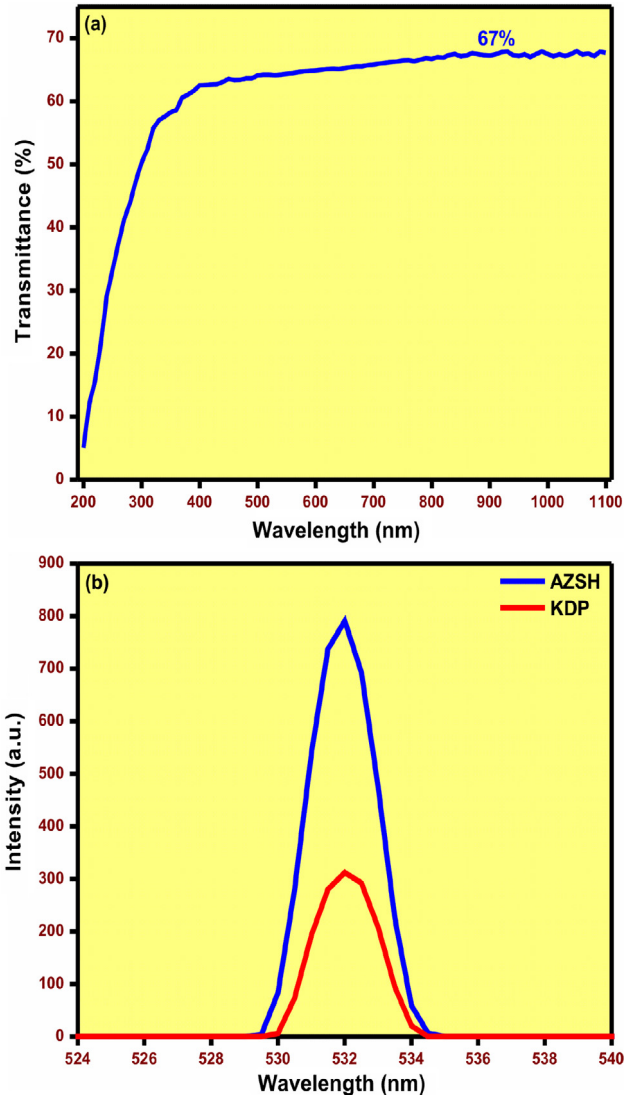

Fig. 2. (a) UV-visible transmittance spectrum. (b) Intensity dependent SHG response.

present analysis the well grown AZSH crystals were selected and powdered to same size micro-granules. The powdered samples of AZSH and reference material KDP were sieved in the quartz cavity and irradiated by the Gaussian filtered beam of Nd:YAG laser. The output window was observed and the emission of bright green light confirmed the prominence of frequency doubling phenomenon in AZSH crystal. The SHG signal was collected through the optical fiber and the intensity dependent response was recorded using the BS-Stellarnet spectrophotometer. The SHG response is graphically represented in Fig. 2b. It reveals that the intensity of AZSH crystal is much higher as compared to KDP and it is found to be 2.53 times higher than that of KDP crystal. In case of typical monoclinic structural orientation of title crystal there is strong possibility of enantiomorphous symmetry which convinces the occurrence of nonlinear optical activity [24–26] in addition to that the unique property of Zn^{2+} ion aids the ligand to ligand charge transfer which is also the key mechanism resulting to remarkably high second order nonlinear response in AZSH crystal [27]. The SHG efficiency of AZSH crystal is exceptionally superior to several inorganic crystals [28–32] currently used for NLO device applications. The SHG efficiency is systematically compared in Table 1.

Table 1
Comparison of SHG efficiency.

Crystal	SHG efficiency	Reference
β-HgBrCl	2.00 (KDP)	[28]
$K_2Al_2B_2O_7$	2.30 (KDP)	[29]
SMTC	1.32 (KDP)	[30]
$Li(H_2O)_4B(OH)_4{\cdot}2H_2O$	0.8 (KDP)	[31]
Hg_2BrI_3	1.2 (KTP)	[32]
AZSH	2.53 (KDP)	Present

The Z-scan technique developed by Bahae et al. [33] is the easiest, benchmark, reliable and sensitive technique to assess the third order nonlinear optical (TONLO) effects flourishing in given material due to interaction with polarized high power laser light intensities. The knowledge of TONLO properties serves a vital purpose to identify the credibility of crystal for optical power limiting, two-photon upconversion lasing, 3D optical data storage, photodynamic therapy, ultrafast optical switching and lithography microscopic designing applications [34,35]. In current investigation the Z-scan studies have been performed using the CW He-Ne laser operating at 632.8 nm. The crystal sample was finely polished to 1 mm thickness and placed at sample holder positioned at the focus (Z = 0) of beam irradiated path. The optical path is sectioned in equal halves by the focus (Z = 0) and in order to record the close aperture Z-scan transmittance curve the samples was translated along the Z-direction. The optical beam transmitted through the crystal was traced with reference to sample position using the detector placed at far field and the Z-scan transmittance curve of AZSH crystal is shown in Fig. 3a. As the optical signal passes through the AZSH crystal it experiences the phase shift about the focus tuning from peak to valley which is classified as negative sign of nonlinear refraction (n_2) [36]. The negative profile of n_2 is identity feature of material inheriting the self-defocusing property [37]. The crystal offers the effect of n_2 which is originated due to incident laser beam intensity of high repetition rate dwelling the thermal lensing effect causing the spacial distribution of optical energy along the crystal surface [38,39]. The on axis phase shift ($\Delta\Phi$) and peak to valley transmittance difference ($\Delta T_{p\text{-}v}$) was calculated using the relation [33],

$$\Delta T_{p-v} = 0.406(1-S)^{0.25}|\Delta\phi| \quad (1)$$

where $S = [1 - \exp(-2r_a^2/\omega_a^2)]$ is the aperture linear transmittance, r_a is the aperture radius and ω_a is the beam radius at the aperture. The magnitude of n_2 was respectively calculated using the equation [33],

$$n_2 = \frac{\Delta\phi}{KI_0L_{eff}} \quad (2)$$

where $K = 2\pi/\lambda$ (λ is the laser wavelength), I_0 is the intensity of the laser beam at the focus (Z = 0), $L_{eff} = [1 - \exp(-\alpha L)]/\alpha$, is the effective thickness of the sample depending on linear absorption coefficient (α) and L thickness of the sample. The n_2 of AZSH crystal is found to be of order 10^{-9} cm^2/W. The AZSH crystal with negative n_2 could be suitable material for optical night vision sensing devices. The open aperture Z-scan configuration is the promising way to examine and calculate the magnitude of TONLO absorption coefficient (β). The Z-scan transmittance curve recorded with open aperture of detector is shown in Fig. 3b. It reveals that as the sample approaches the focus position the crystal allows maximum transmittance which confirms the occurrence of saturable absorption (SA) effect [40] in AZSH crystal. The SA effect typically evolves due to dominance of ground state linear absorption over the excited stated absorption [41]. The magnitude of β was thus calculated using the equation [33],

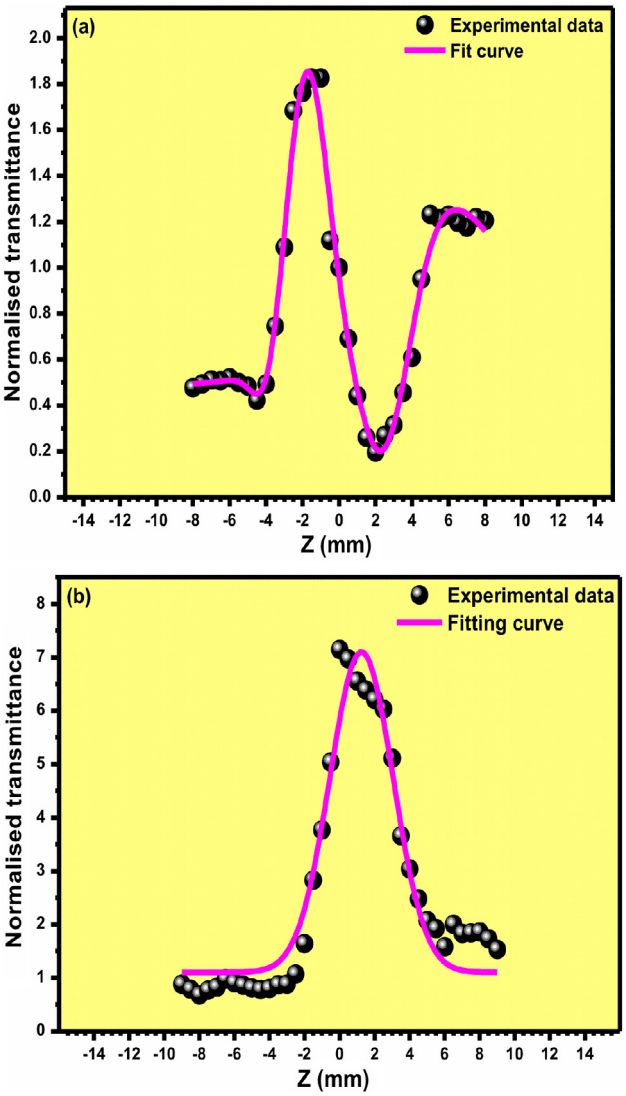

Fig. 3. Z-scan transmittance curve with aperture (a) close and (b) open.

$$\beta = \frac{2\sqrt{2}\Delta T}{I_0 L_{eff}} \tag{3}$$

where ΔT is the one valley value at the open aperture Z-scan curve. The β magnitude of AZSH crystal was found to be in order of 10^{-4} cm/W. The TONLO susceptibility (χ^3) is most essential parameter to determine the polarizing ability of the material [42] and thus the χ^3 was evaluated by solving the given relations [33],

$$Re\chi^{(3)}(esu) = 10^{-4}(\varepsilon_0 C^2 n_0^2 n_2)/\pi \ (\mathrm{cm}^2/\mathrm{W}) \tag{4}$$

$$Im\chi^{(3)}(esu) = 10^{-2}(\varepsilon_0 C^2 n_0^2 \lambda\beta)/4\pi^2 \ (\mathrm{cm/W}) \tag{5}$$

$$\chi^{(3)} = \sqrt{(Re\chi^{(3)})^2 + (Im\chi^{(3)})^2} \tag{6}$$

where ε_0 is the vacuum permittivity, n_0 is the linear refractive index of the sample and c is the velocity of light in vacuum. The χ^3 of AZSH crystal is found to be of order 10^{-4} esu which is appreciably high. The TONLO parameters of AZSH crystal are highlighted with literature in Table 2.

The crystals that can sustain high power laser shots for longer span without damage can undoubtedly find its importance for manufacturing laser assisted photonics devices which justify the fact that determination of laser damage threshold (LDT) is vital aspect. The LDT of the AZSH crystal has been assessed in multishot mode by focusing the polarized beam of pulse mode operated Nd: YAG laser (1064 nm, 10 ns, 10 Hz). The beam of 1 mm diameter was focused on the defect less and plane surface of AZSH crystal sample using the converging lens of focal length 35 cm and each shot was maintained for 30 s. The surface was shot by attenuating the beam energy till the crystal show prominent damage. The AZSH crystal showed major damage at energy of 131.4 mJ which was also confirmed by the sound of crack. The witnessed damage was captured in reflection mode and the microimage of damage is shown in Fig. 4a. The LDT was calculated using the relation $P = E/\tau\pi r^2$, where E is the energy at which crystal showed damage, τ is the pulse width and r is the radius of the damage. The laser induced damage in crystal is nucleated due to several complex effects such as electron avalanche breakdown, nonlinear absorption, stimulated Brillion scattering, thermally induced localized photoionization and it is influenced by the laser parameters (repetition rate, incident beam spot size, polarization mode) as well [43–45]. The photoionization of focused crystal site driven by thermal effect is more dominant phenomenon when dealing with nanosecond time scale lasers [46] thus the surface damage is caused in the form of breakage, cracking, solidification, fusion, melting and decomposition of the material [47]. The LDT of AZSH crystal is thus found to be 345.57 MW/cm^2.

Table 2
TONLO parameters.

Crystal	n_2 (cm^2/W)	β (cm/W)	χ^3 (esu)	Reference
KH_2PO_4	1.16×10^{-5}	1.06×10^{-5}	2.75×10^{-4}	[13]
α-$LiIO_3$	5.46×10^{-7}	3.95	1.63×10^{-3}	[40]
AZSH	-2.16×10^{-9}	1.25×10^{-4}	3.03×10^{-4}	Present

The knowledge of dielectric constant and dielectric loss is most essential when designing the electro-optic and microelectronics devices. Thus the frequency response of dielectric constant and dielectric loss of AZSH crystal is shown in Fig. 4b. The dielectric constant is driven by the electronic, ionic, orientation and space charge polarization mechanisms [48]. The AZSH crystal contributes high dielectric constant at low frequency domain as all four polarization mechanisms are active while the dielectric constant reaches to saturation state in high frequency region as polarization activity is less responsive to high frequency of applied electromagnetic field [49]. The attribution of low dielectric constant by AZSH crystal at high frequencies indicates that it is capable of delivering less power consumption and reduced Rc delay [50]. In addition the Millers rule suggest that the material with low dielectric constant can deliver high SHG efficiency [51] which is very true in case of AZSH crystal. Thus the typical characteristic of low dielectric constant of AZSH crystal might be an important asset for designing photonics, THz wave generation, microelectronics, optoelectronics, broadband electro-optic modulators and field detection devices [52,53]. The effect of dielectric loss originates due to physical parameters such as defects (voids, vacancies, pores, striations, impurities, inclusions) and random surface orientation in the crystal which impede the propagation of electromagnetic signal and give rise to successive loss of signal in the form of heat [54]. The dielectric loss of AZSH crystal significantly decreases with increase in frequency which confirms that the grown crystal possesses good optical quality and lesser electrically active defects [55]. The AZSH crystal with promising dielectric parameters is desirable parameter for wide range of applications.

The photoluminescence (PL) is the peculiar feature that aids to examine the impurity level and transition of electron to different energy states in given material by tracing the trajectory of the electron during photo-relaxation. The electron during its transition to

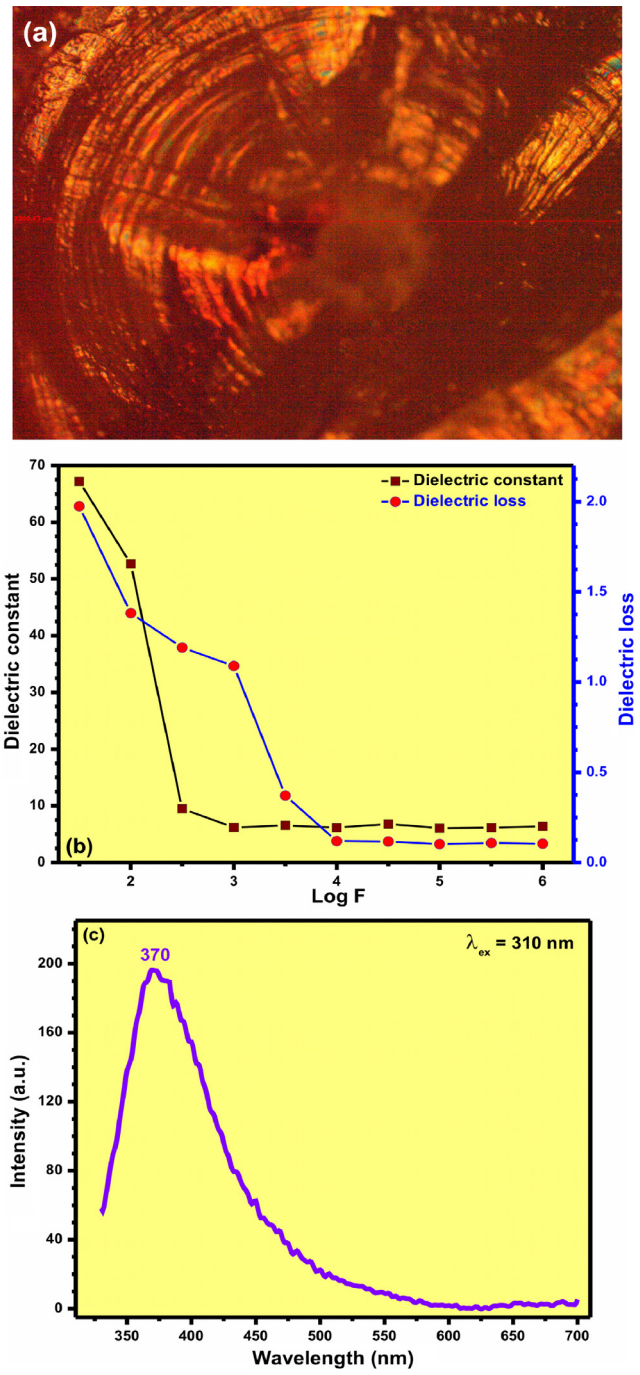

Fig. 4. (a) Pattern of laser damage crystal surface. (b) Frequency dependent dielectric response. (c) PL emission spectrum of AZSH crystal.

ground state losses its energy in the form of electromagnetic radiates and evaluation of this radiation in visible region is of vital importance for photonic crystal to propose its utility in biomedical and chemical applications [56,57]. The AZSH crystal material has been photo-excited at an energy wavelength of 310 nm and the PL emission spectrum was recorded in the range of 330–700 nm. It is observed that the AZSH crystal attributes the single peak maxima centered at 370 nm which determines the prominence of violet colored emission. The absence of intermediate transition peaks and single colored emission confirms the electronic purity of AZSH crystal.

In crystals grown by solvent evaporation technique the nucleation of in-grown defects (defect structures comprising growth sector boundaries, solvent inclusions, growth band, slip band, grain boundaries, dislocations, vacancies, cracks, stacking faults, etc) occurs due to spontaneous variations in the growth conditions and these defects largely hamper the performance of crystal [58,59]. As far as defects study is concerned the chemical etching is one of the simplest but effective technique which serves the purpose to identify the dimensional origin of defects [60], evaluate the distribution of defects [61], pattern of defect symmetry (triangular, spiral, hillocks, oval, rectangular, pyramidal, square, etc) [62] and growth habitat [63] associated with the crystal. It is resolved that the behavior of the etching surface depends on three crucial factors (a) selection of etchant, (b) reaction rate of etchant with selected

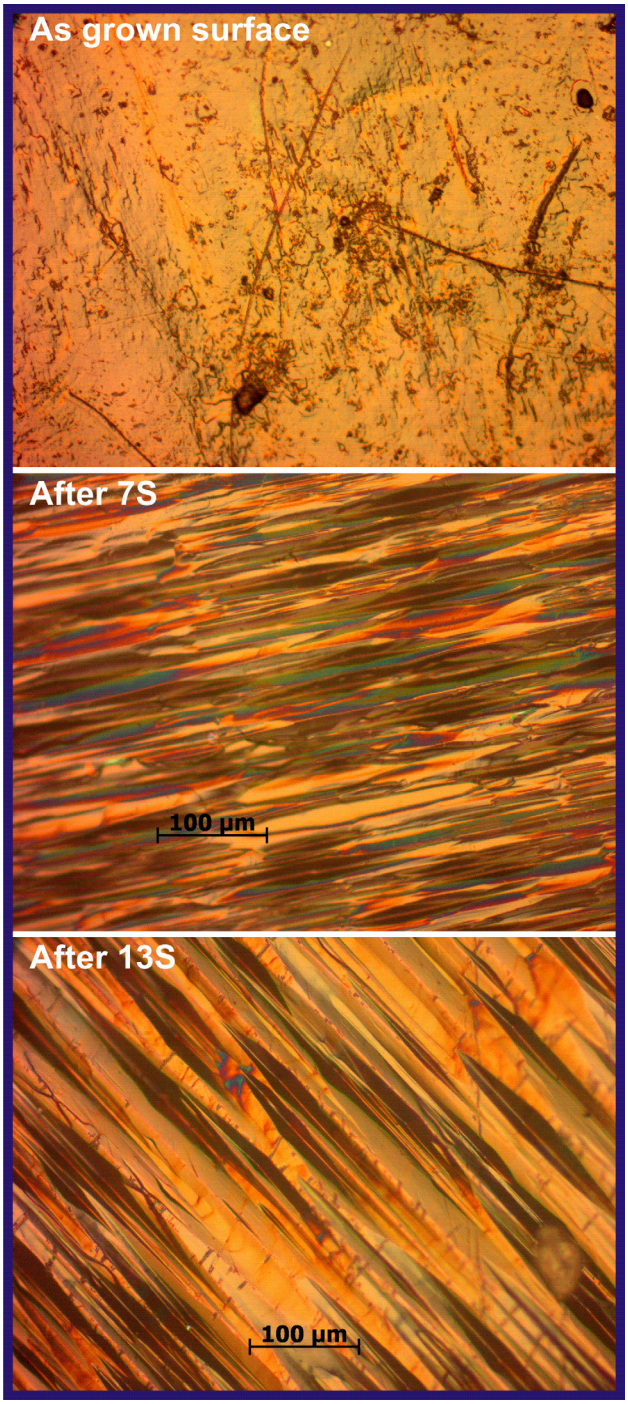

Fig. 5. Etch pattern of AZSH crystal surface.

plane of crystal and (c) time for which etchant is allowed to interact with surface [64]. As dislocation sites are sensitive to the suitable etchant in present analysis the AZSH crystal was etched with water and the etch pattern were recorded in reflection mode as shown in Fig. 5. It is observed that the surface without etching shows randomly distributed pits and striations however as the surface was etched with water it uncovers systematically oriented etch pattern. The microimage captured after 7 s reveals the intermixed etch pattern which might have been observed due to segregation of impurities. Further etching for 13 s reveals the clear picture of etch pits which are evenly distributed along the crystal surface and appear quite dark. The darkness indicate that the etch pits are fairly deep due to which the reflected light gets trapped and does not reach the microscope tube. The etch pit density (EPD) of AZSH crystal is found to be 9.6×10^3 cm^{-2}.

4. Conclusion

The promising inorganic NLO AZSH single crystal has been successfully grown by slow solvent evaporation technique. The cell dimensions and space group of AZSH crystal has been determined by means of single crystal XRD technique and the good crystalline nature has been confirmed by powder XRD analysis. The UV–visible studies revealed that the AZSH crystal has wide optical transparency window with transmittance of 67% within the wavelength range of 200–1100 nm. The promising NLO behavior of AZSH crystal has been confirmed by Kurtz-Perry test and Z-scan analysis. The SHG efficiency of AZSH crystal is found to be 2.53 times higher than KDP crystal which is proposed to be flourished due to enantiomorphous crystal orientation and effective ligand to ligand charge transfer ability of Zn^{2+} ion. He-Ne laser (632.8 nm) beam irradiation inculcated negative nonlinear refraction and saturable absorption effect in AZSH crystal. The n_2, β and χ^3 of AZSH crystal is found to be -2.16×10^{-9} cm^2/W, 1.25×10^{-4} cm/W, 3.03×10^{-4} esu respectively. The 1064 nm Nd:YAG laser induced surface damage threshold of AZSH crystal is found to be 345.57 MW/cm^2. The AZSH crystal has been scanned within 330–700 nm which revealed the single peak at 370 nm indicating the prominence of violet colored emission. The dielectric analysis uncovered the low dielectric nature of AZSH crystal which established it as suitable material for application at higher frequencies. The etching study revealed the oriented growth habitat of AZSH crystal with EPD of magnitude 9.6×10^3 cm^{-2}. The AZSH crystal with promising optical, dielectric and microscopic properties is advised as potential alternative candidate for designing electro-optic modulators, microelectronics, optical switching and laser assisted photonic devices.

Acknowledgements

Author Mohd Anis is thankful to UGC, New Delhi, India for awarding the Maulana Azad National Fellowship [F1-17.1/2015-16/MANF-2015-17-MAH-68193]. Authors acknowledge RUSA Centre, Dr. Babasaheb Ambedkar Marathwada University, Aurangabad (MAH), India for Powder XRD analysis. Author G.G. Muley is thankfull to DST-SERB, India for the sanctioning major project (SB/EMEB-328/2013). Author Mohd Shkir would like to express his gratitude to RCAMS-King Khalid University, Saudi Arabia for support.

References

[1] Maierhaba Abudoureheman, Li Wang, Xianming Zhang, Yu. Hongwei, Zhihua Yang, Chen Lei, Jian Han, Shilie Pan, Inorg. Chem. 54 (2015) 4138–4142.
[2] Maierhaba Abudoureheman, Shujuan Han, Ying Wang, Bing-Hua Lei, Zhihua Yang, Shilie Pan, Inorg. Chem. 56 (2017) 3939–3945.
[3] R.N. Shaikh, Mohd Anis, M.D. Shirsat, S.S. Hussaini, J. Optoelectron. Adv. Mater. 16 (2014) 1147–1152.
[4] F.Q. Li, N. Zong, F.F. Zhang, J. Yang, F. Yang, Q.J. Peng, D.F. Cui, J.Y. Zhang, X.Y. Wang, C.T. Chen, Z.Y. Xu, Appl. Phys. B 108 (2012) 301–305.
[5] S.P. Ramteke, Mohd Anis, M.I. Baig, Mohd Shkir, V. Ganesh, G.G. Muley, Optik 158 (2018) 634–638.
[6] David N. Nikogosyan, Nonlinear Optical Crystals: A Complete Survey, Springer, New York, 2005.
[7] L. Robert, Bryer Annual Review, Mater. Sci. 4 (1974) 147–190.
[8] A. Abu El-Fadl, A.M. Nashaat, Appl. Phys. A 123 (2017) 339–349.
[9] S.P. Ramteke, Mohd Anis, M.I. Baig, G.G. Muley, Optik 154 (2018) 275–279.
[10] Mohd Anis, M.S. Pandian, M.I. Baig, P. Ramasamy, G.G. Muley, Mater. Res. Innov. (2017), https://doi.org/10.1080/14328917.2017.1329992.
[11] G. Ramasamy, G. Bhagavannarayana, G. Madhurambal, Subbiah Meenakshisundaram, J. Cryst. Growth 352 (2012) 137–142.
[12] Frederick Wooten, Optical Properties of Solids, Academia Press, New York, 1972.
[13] M.I. Baig, Mohd Anis, G.G. Muley, Opt. Mater. 72 (2017) 1–7.
[14] William D. Callister, Materials Science and Engineering: An Introduction, John Wiley & Sons, New York, 2007.
[15] Mohd Anis, S.P. Ramteke, M.D. Shirsat, G.G. Muley, M.I. Baig, Opt. Mater. 72 (2017) 590–595.
[16] Michael Bass, Handbook of Optics, second ed., vol. 2, Mc-Graw Hill, USA, 1995 (Chapter 33).
[17] Mohd Anis, S.S. Hussaini, Mohd Shkir, S. AlFaify, M.I. Baig, G.G. Muley, Optik 157 (2018) 592–596.
[18] Min-Hua Jiang, Qi Fang, Adv. Mater. 11 (1999) 1147–1151.
[19] Hans P. Glick, Materials Science Research Horizons, Nova Science, New York, 2007.
[20] Neeti Goel, Nidhi Sinha, Binay Kumar, Opt. Mater. 35 (2013) 479–486.
[21] Mohd Anis, G.G. Muley, M.I. Baig, S.S. Hussaini, M.D. Shirsat, Mater. Res. Innov. 21 (2017) 439–446.
[22] V.G. Pahurkar, Mohd Anis, M.I. Baig, S.P. Ramteke, B. Babu, G.G. Muley, Optik 142 (2017) 421–425.
[23] S.K. Kurtz, T.T. Perry, J. Appl. Phys. 39 (1968) 3798–3813.
[24] Richard J.D. Tilley, Crystals and Crystals Structures, John Wiley & Sons, England, 2006, p. 76.
[25] Venkatram Nalla, Raghavender Medishetty, Yue Wang, Zhaozhi Bai, Handong Sun, Ji. Weid, J.J. Vitta, IUCr JCryst. Eng. 2 (2015) 317–321.
[26] E.W. Meijer, E.E. Havinga, G.L.J.A. Rikken, Phys. Lett. Rev. 65 (1990) 37–39.
[27] G. Pascal, Lacroix, Chem. Mater. 8 (1996) 541–545.
[28] Yangyang Dang, Xianggao Meng, Kui Jiang, Cheng Zhong, Xingguo Chena, Jingui Qin, Dalton Trans. 42 (2013) 9893–9897.
[29] B. Milton Boaz, S. Mary Navis Priya, J. Mary Linet, P. Martin Deva Prasath, S. Jerome Das, Opt. Mater. 29 (2007) 827–832.
[30] M. Packiya Raja, S.M. Ravi Kumar, R. Srineevasan, R. Ravisankar, J. Taibah Uni. Sci. 11 (2017) 76–84.
[31] Yaqin Liu, Zhaohui Chen, Zhizhong Zhang, Ying Wang, Xiaoyu Dong, Zhihua Yang, Mater. Res. Bull. 83 (2016) 423–427.
[32] Yanjun Li, Meng Wang Tianxiang Zhu, Xianggao Meng, Cheng Zhong, Xingguo Chena, Jingui Qin, Dalton Trans. 41 (2012) 763–766.
[33] M.S. Bahae, A.A. Said, T.H. Wei, D.J. Hagan, E.W.V. Stryland, IEEE J. Quant. Electron. 26 (1990) 760–769.
[34] Ting Bin Li, Ya Li Hu, Chun Lin Ma, Guo Fang He, Ren Gao Zhao, Guo Bing Zhen, Appl. Organometal. Chem. 25 (2011) 867–870.
[35] R.N. Shaikh, Mohd Anis, M.D. Shirsat, S.S. Hussaini, Optik 154 (2018) 435–440.
[36] A. Aditya Prasad, S. Kalainathan, S.P. Meenakshisundaram, Optik 127 (2016) 6134–6149.
[37] X.B. Sun, X.Q. Wang, Q. Ren, G.H. Zhang, H.L. Yang, L. Feng, Mater. Res. Bull. 41 (2006) 177–182.
[38] Gu. Bing, Hui-Tian Wang, Wei Ji, Opt. Lett. 34 (2009) 2769–2771.
[39] S.P. Ramteke, Mohd Anis, M.S. Pandian, S. Kalainathan, M.I. Baig, P. Ramasamy, G.G. Muley, Opt. Laser Technol. 99 (2018) 197–202.
[40] R. Ashok Kumar, R. Ezhil Vizhi, N. Vijayan, G. Bhagavannarayana, D. Rajan-Babu, J. Pure Appl. Ind. Phys. 1 (2010) 61–67.
[41] K. Nivetha, S. Kalainathan, M. Yamada, Y. Kondo, F. Hamada, J. Mater. Sci.: Mater. Electron. 28 (2017) 5180–5191.
[42] Richard Haglund, F. Trager, Springer Handbook of Lasers and Optics, Springer, New York, 2007.
[43] Hidetsugu Yoshida, Hisanori Fujita, Masahiro Nakatsuka, Masashi Yoshimura, Takatomo Sasaki, Tomosumi Kamimura, Kunio Yoshida, Jpn. J. Appl. Phys. 45 (2006) 766–769.
[44] M.I. Baig, M. Anis, S. Kalainathan, B. Babu, G.G. Muley, Mater. Technology: Adv. Perform. Mater. 32 (2017) 560–568.
[45] S.M. Azhar, S.S. Hussaini, M.D. Shirsat, G. Rabbani, Mohd Shkir, S. Alfaify, H.A. Ghramh, M.I. Baig, Mohd Anis, Mater. Res. Innov. (2017), https://doi.org/10.1080/14328917.2017.1392694.
[46] S. Vanishri, J.N. Babu Reddy, H.L. Bhat, S. Ghosh, Appl. Phys. B 88 (2017) 457–461.
[47] J.N. Babu Reddy, S. Vanishri, Ganesh Kamath, Suja Elizabeth, H.L. Bhat, D. Isakov, M. Belsley, E. de Matos Gomes, T.L. Aroso, J. Cryst. Growth 311 (2009) 4044–4049.
[48] Brian S. Mitchell, An Introduction to Materials Engineering and Science, John Wiley & Sons, Hoboken, New Jersey, 2004, p. 566.
[49] S.M. Azhar, Mohd Anis, S.S. Hussaini, S. Kalainathan, M.D. Shirsat, G. Rabbani, Mater. Sci.-Poland 34 (2016) 800–805.

[50] B.D. Hatton, K. Landskron, W.J. Hunks, M.R. Bennett, D. Shukaris, D.D. Perovic, G.A. Ozin, Mater. Today 9 (2006) 22–31.
[51] R.C. Miller, Appl. Phys. Lett. 5 (1964) 17–19.
[52] Y.B. Rasal, Mohd Anis, M.D. Shirsat, S.S. Hussaini, Mater. Res.Innov. (2017), https://doi.org/10.1080/14328917.2017.1327199.
[53] Mohd Anis, G.G. Muley, V.G. Pahurkar, M.I. Baig, S.R. Dagdale, Mater. Res. Innov. 22 (2018) 99–106.
[54] Mohd Anis, G.G. Muley, Opt. Laser Technol. 90 (2017) 190–196.
[55] R.N. Shaikh, Mohd Anis, G. Rabbani, M.D. Shirsat, S.S. Hussaini, Optoelectron. Adv. Mater. – Rapid Commun. 10 (2016) 526–531.
[56] R.N. Shaikh, M. Anis, M.D. Shirsat, S.S. Hussaini, Mater. Technol Adv. Perform. Mater. 19 (2015) 187–191.
[57] Timothy H. Gfroerer, Photoluminescence in Analysis of Surfaces and Interfaces, Encyclopedia of Analytical Chemistry, John Wiley & Sons Ltd., Chichester, 2000, pp. 9209–9231.
[58] Mohd Anis, M.I. Baig, M.S. Pandian, P. Ramasamy, S. AlFaify, V. Ganesh, G.G. Muley, H.A. Ghramh, Cryst. Res. Technol (2018), https://doi.org/10.1002/crat.201700165.
[59] V. Sivasubramani, Mohd Anis, S.S. Hussaini, G.G. Muley, M. Senthil Pandian, P. Ramasamy, Mater. Res. 21 (2017) 426–433.
[60] Eugene A. Irene, Electronic Materials Science, John Wiley & Sons, New Jersey, 2005, pp. 61–62.
[61] M. Lydia Caroline, S. Vasudevan, Mater. Chem. Phys. 113 (2009) 670–674.
[62] M.A. Gosalvez, R.M. Nieminen, New J. Phys. 5 (2003) 100.1–100.28.
[63] M. Rajalakshmi, R. Indirajith, P. Ramasamy, R. Gopalakrishnan, Mol. Cryst. Liq. Cryst. 548 (2011) 126–141.
[64] K. Sangwal, Etching of crystals: Theory, Experiment and Application: Defects in Solids, North-Holland, Amsterdam, The Netherlands, 1987.